

Atypical relationships between spontaneous EEG and fMRI activity in autism

Lisa E. Mash^{1,2}, Brandon Keehn³, Annika C. Linke¹, Thomas T. Liu⁴, Jonathan L. Helm^{2,5},
Frank Haist^{2,6}, Jeanne Townsend^{2,7}, Ralph-Axel Müller^{1,2}

¹ Brain Development Imaging Laboratories, Department of Psychology, San Diego State University, 6363 Alvarado Ct., Suite 200, San Diego, CA, 92120, United States

² San Diego State University/University of California San Diego Joint Doctoral Program in Clinical Psychology, 6363 Alvarado Ct., Suite 103, San Diego, CA, 92120, United States

³ Department of Speech, Language, and Hearing Sciences, Purdue University, 715 Clinic Drive, Lyles-Porter Hall, West Lafayette, IN, 47907, United States

⁴ Center for Functional MRI, Department of Radiology, University of California, San Diego, 9500 Gilman Dr. #0677, La Jolla, CA, 92093, United States

⁵ Department of Psychology, San Diego State University, 5500 Campanile Dr., San Diego, CA, 92182, United States

⁶ Department of Psychiatry, University of California, San Diego, 9500 Gilman Dr., #0115, La Jolla, CA, 92093, United States

⁷ Department of Neurosciences, University of California, San Diego, 8950 Villa La Jolla Dr., Ste 216-B, La Jolla, CA, 92037, United States

Email: lisa.e.mash@gmail.com; bkeehn@purdue.edu; annikalinke@gmail.com;
ttliu@ucsd.edu; jhelm@sdsu.edu; fhaist@ucsd.edu; jtownsend@ucsd.edu;
rmueller@sdsu.edu

Running title: EEG-fMRI in ASD

Keywords: Autism, Functional MRI, EEG, Alpha, Resting State

This paper has been peer-reviewed and accepted for publication, but has yet to undergo copyediting and proof correction. The final published version may differ from this proof.

Brain Connectivity
Atypical relationships between spontaneous EEG and fMRI activity in autism (DOI: 10.1089/brain.2019.0693)

Downloaded by Imperial College School Of Med from www.liebertpub.com at 01/02/20. For personal use only.

Corresponding Author:

Ralph-Axel Müller

Brain Development Imaging Laboratories, Department of Psychology

San Diego State University, 6363 Alvarado Ct., Suite 200, San Diego, CA 92120

Phone: 619-594-5276

Email: rmueller@sdsu.edu

Abstract

Autism spectrum disorders (ASDs) have been linked to atypical communication among distributed brain networks. However, despite decades of research, the exact nature of differences between typically developing (TD) individuals and those with ASDs remains unclear. ASDs have been widely studied using resting state neuroimaging methods, including both functional MRI (fMRI) and electroencephalography (EEG). However, little is known about how fMRI and EEG measures of spontaneous brain activity are related in ASDs. In the current study, two cohorts of children and adolescents underwent resting-state EEG ($n = 38$ per group) or fMRI ($n = 66$ ASD, 57 TD), with a subset of individuals in both the EEG and fMRI cohorts ($n = 17$ per group). In the EEG cohort, occipito-parietal EEG alpha power was found to be reduced in ASDs. In the fMRI cohort, blood oxygen level-dependent (BOLD) power was regionally increased in right temporal regions and there was widespread overconnectivity between thalamus and cortical regions in the ASD group relative to the TD group. Finally, multimodal analyses found that while TD children showed consistently positive relationships between EEG alpha power and regional BOLD power, these associations were weak or negative in ASDs. These findings suggest atypical links between alpha rhythms and regional BOLD activity in ASDs, possibly implicating neural substrates and processes that coordinate thalamocortical regulation of the alpha rhythm.

Keywords: Autism, Functional MRI, EEG, Alpha, Resting State

Acronyms

ABIDE	Autism Brain Imaging Data Exchange
AFNI	Analysis of Functional Neuroimages
ASDs	Autism spectrum disorders
BOLD	Blood oxygen level-dependent
EEG	Electroencephalography
(f)ALFF	(Fractional) amplitude of low frequency fluctuations
FC	Functional connectivity
FD	Framewise displacement
fMRI	Functional magnetic resonance imaging
FSL	FMRIB Software Library
FWHM	Full width at half-maximum
GSR	Global signal regression
ICA	Independent component analysis
MEG	Magnetoencephalography
MLM	Multilevel modeling
MNI	Montreal Neurological Institute
RMSD	Root mean squared displacement
ROI	Region of interest
TD	Typically developing

Introduction

Autism spectrum disorders (ASDs) are neurodevelopmental disorders defined behaviorally by social communication deficits and the presence of restricted/repetitive patterns of behavior or interest (American Psychiatric Association 2013). It is currently estimated that one in 59 eight-year-olds in the United States are on the autism spectrum (Baio et al. 2018). However, the neurobiological basis of these disorders remains poorly understood. Research clarifying the nature of brain differences in ASDs may improve treatment and diagnostic strategies and is therefore a high priority.

Over the past several decades, interest in brain functioning in ASDs has grown rapidly. Studies using functional MRI (fMRI) and electroencephalography (EEG) to examine neural activity in vivo comprise the majority of this literature. While fMRI research broadly supports atypical coordination (i.e., functional connectivity; FC) across distributed brain networks in ASDs, there have been mixed and sometimes conflicting reports of underconnectivity and overconnectivity involving numerous regions and functional networks (Di Martino et al. 2014, Hull et al. 2016). However, findings of atypical thalamocortical circuitry have been relatively consistent, with multiple studies reporting overconnectivity between thalamus and sensorimotor cortical regions (Cerliani et al. 2015, Nair et al. 2015, Woodward et al. 2017). These findings are further supported by evidence of structural thalamic differences in ASDs (Schuetze et al. 2016). Much like the fMRI literature, EEG studies have produced mixed results with respect to both power and coherence across a range of frequencies (Wang et al. 2013, O'Reilly et al. 2017). Despite these inconsistencies, one of the best replicated findings in ASDs is decreased power in the alpha frequency band (i.e., 8-12 Hz) at rest (Dawson et al. 1995, Chan et al. 2007, Murias et al. 2007, Sheikhan et al. 2012, Tierney et al. 2012, Keehn et al. 2017).

To date, there has been little progress relating findings across modalities in ASDs (Mash et al. 2018), and it is currently unknown how reports of reduced EEG alpha power and atypical thalamocortical activity may be associated. While EEG directly measures postsynaptic potentials (Niedermeyer et al. 2011, Supek and Aine 2014), fMRI detects the blood oxygen level-dependent (BOLD) signal, an indirect measure of neural activity influenced by vascular and metabolic factors (Hillman 2014). Therefore, measures of

magnitude (i.e., power) and synchronicity (i.e., FC) derived from different modalities may reflect neuronal communication in fundamentally different ways. Studies combining both modalities in the same individuals allow for joint analysis and direct comparison of EEG and fMRI results.

In typically developing (TD) adults, a large body of simultaneous EEG-fMRI work has consistently demonstrated that spontaneous EEG alpha power is positively associated with thalamic BOLD activity (Goldman et al. 2002, de Munck et al. 2007, Bridwell et al. 2013) and negatively related to cortical BOLD activity (Goldman et al. 2002, Laufs et al. 2003, Olbrich et al. 2009, Bridwell et al. 2013). The relationship between EEG alpha power and BOLD FC is less well established; however, there is some evidence that increased EEG alpha power is associated with reduced anticorrelation (i.e., less negative correlations) between thalamic and cortical regions (Scheeringa et al. 2012, Allen et al. 2018). Multimodal imaging research in ASDs remains very limited. To our knowledge, only two small EEG-fMRI studies in ASDs have been published, both of which explored neural processing during auditory and language processing tasks using concurrent EEG-fMRI (Jochaut et al. 2015, Hames et al. 2016). While these efforts provide first glimpses of potential links between electrophysiological and hemodynamic measures during task performance in ASDs, they cannot speak to unimodal resting state findings involving EEG alpha power and thalamocortical networks.

To our knowledge, there are currently no published resting state EEG-fMRI studies of ASDs. However, established relationships between thalamocortical networks and EEG alpha power in typical development described above provide a compelling direction for future ASD research combining EEG and fMRI. Although there are advantages to simultaneous data acquisition, this procedure is often lengthy and uncomfortable. This is especially problematic for children with developmental disorders. Separately acquired EEG-fMRI data cannot speak to concurrent fluctuations in regional BOLD activity/coordination and EEG alpha power within individuals. However, these data may still provide important insight into multimodal relationships between individuals.

In order to investigate links between separately acquired EEG and fMRI, suitable summary measures for EEG alpha power, BOLD activity, and BOLD FC must be selected. EEG alpha power can be averaged over an acquisition period to yield a specific value for each participant. Calculating a single BOLD FC value over an entire scan period for an individual, on the other hand, is challenging as BOLD units are arbitrary and only relative BOLD activity changes can be interpreted meaningfully. Therefore, spontaneous BOLD activity (i.e., power) is best summarized by the amplitude of low frequency fluctuations (ALFF; Zang et al. 2007), a measure that captures power in BOLD frequencies typically around .01-.1 Hz. ALFF is often reported together with fractional ALFF (fALFF), i.e., the ratio between low frequency power and total power of all frequencies (Zou et al. 2008), as ALFF tends to have better test-retest reliability, whereas fALFF is considered more robust to non-neuronal artefact (Zuo et al. 2010). However, ALFF/fALFF has only played a minimal role in the ASD neuroimaging literature to date. A few relevant studies have reported varying findings, from broadly increased ALFF (Supekar et al. 2013) to regionally increased fALFF in right frontal and temporal regions (Di Martino et al. 2014) and decreased fALFF in occipital regions (Di Martino et al. 2014, Itahashi et al. 2015)

The primary aims of this study were to 1) clarify previous unimodal EEG and fMRI findings in ASDs described above, and 2) to establish inter-individual relationships between EEG alpha power and thalamic activity, cortical activity, and thalamocortical FC in a sample of adolescents with and without ASDs.

Materials and Methods

Participants

Resting-state EEG was collected from 76 individuals (38 ASD, 38 TD) ages 7-18 years. Groups did not significantly differ with respect to age, handedness, sex, nonverbal IQ, or EEG length after preprocessing (Table 1a). None of the TD participants were taking psychotropic medications or had any documented history of psychiatric or developmental disorders. In the ASD group, medication status was documented for 23 of 38 individuals. Of these, six reported taking psychotropic medications.

Functional MRI data were separately acquired from 123 individuals (66 ASD, 57 TD) ages 6-18 years. ASD and TD groups did not significantly differ with respect to age, handedness, sex, nonverbal IQ, RMSD, or in-scanner head motion (Table 1b). As in the EEG sample, none of the TD participants were taking psychotropic medications or had any documented history of psychiatric or developmental disorders. In the ASD group, 23 individuals reported taking psychotropic medications, 37 were unmedicated, and medication status was undocumented for six individuals.

A subset of participants underwent fMRI and EEG acquisition within three months of one another (22 ASD, 25 TD, ages 12-17 years; Table 1c). Four individuals with ASDs and six typically developing individuals were excluded from multimodal analyses due to excessive fMRI artefact. One individual with ASD was excluded due to an incidental finding on MRI. Two additional typically developing individuals were excluded from the multimodal sample to improve matching and to maintain equal sample sizes. The final EEG-fMRI sample consisted of 17 individuals per group with high-quality data in both modalities. Of these participants, six ASD participants were prescribed medications and the remaining 11 were unmedicated. All available medication and comorbidity data are summarized in Table S1.

Across all samples, ASD diagnoses were confirmed based on the Autism Diagnostic Interview–Revised (ADI-R, Lord, Rutter, & Le Couteur, 1994), the Autism Diagnostic Observation Schedule- Generic (ADOS-G; Lord et al. 2000) or Autism Diagnostic Observation Schedule, Second Edition (ADOS-2; Gotham et al. 2007), and expert clinical judgment according to DSM-5 criteria. The Wechsler Abbreviated Scales of Intelligence (WASI, Wechsler, 1999) or Wechsler Abbreviated Scales of Intelligence, Second Edition (WASI-II, Wechsler, 2011) was administered to all participants. Informed assent and consent were obtained from all participants and caregivers in accordance with the University of California, San Diego and San Diego State University Institutional Review Boards.

Electroencephalography (EEG)

Acquisition

Continuous EEG was recorded using a Biosemi ActiveTwo system with 68 Ag/AgCl active electrodes. Sixty-four electrodes were mounted in an elastic cap according to locations in the modified International 10–20 system. Remaining electrodes were placed below the right eye, on the outer canthus of the left eye (to monitor blinks and saccades), and over the left and right mastoids (reference). EEG data were recorded at a sampling rate of 256Hz and DC offsets were kept below 25 mV at all channels. Participants completed six minutes of eyes-open EEG, during which a black central fixation crosshair was presented on a grey background. Participants were instructed to relax, remain as still as possible, and look at the crosshair.

Data Processing

Data were processed in EEGLAB (Delorme and Makeig 2004) high-pass filtered at 1 Hz, and re-referenced to the grand average. ICA components were applied using the Fieldtrip toolbox (Oostenveld et al. 2011). Each participant's component activations were first visually inspected for motor artifact, and noisy segments were manually rejected. Component activations and their scalp maps were then examined to identify ocular artifacts, and artifact-contaminated components were removed (Jung et al. 2000, Jung et al. 2000). Finally, noisy channels were excluded and replaced as missing values. After preprocessing, all participants had at least two minutes of remaining data for subsequent analyses (Table 1a, Table 1c). For each channel, a fast Fourier transform (EEGLab's spectopo) was applied to continuous (unepoched) data to determine the magnitude of power at frequencies ranging from .25 to 128 Hz, at .25 Hz increments. The spectral power values were converted from decibels to microvolts squared (μV^2).

Alpha Power Analysis

Alpha power, expressed as microvolts squared (μV^2) was extracted from and averaged across parieto-occipital (Oz, POz, O1, O2, PO3, PO4) electrodes. There is strong evidence

that peak alpha frequency varies substantially between individuals (Haegens et al. 2014), shifts throughout childhood and adolescence (Cragg et al. 2011, Miskovic et al. 2015), and may differ between ASDs and typical development (Edgar et al. 2015, Dickinson et al. 2018). Therefore, it has been recommended that alpha frequency windows be individually defined for each participant (Klimesch 1999). For this study, the alpha peak was defined as the local maximum of the average parieto-occipital power spectrum between 7-13 Hz. Because the alpha rhythm is most prominent in posterior regions (Britton et al. 2016), only parieto-occipital electrodes were used to optimize signal-to-noise and improve peak estimates. Occipito-parietal alpha power (referred to henceforth as “alpha power”) was then extracted from the 4-Hz window surrounding this midpoint (e.g., a participant with an alpha peak at 9 Hz will have an alpha window of 7-11 Hz). For participants with no clear alpha peak ($n = 7$, all ASD), a standard window of 8-12 Hz was applied. Individual alpha peaks ranged from 7.5 Hz to 12.5 Hz and did not differ significantly between groups (ASD mean (sd) = 9.76 (.87) Hz, TD mean (sd) = 9.80 (.73) Hz, $p = .82$).

Absolute and relative parieto-occipital alpha power were compared between groups using two-sample t-tests with degrees of freedom adjusted for unequal variances (using Satterthwaite’s approximation). These group analyses were repeated on an unmedicated subsample of ASD participants and a matched TD group. To ensure that our findings were not primarily due to differences in individual alpha windows, a standard alpha window of 8-12 Hz was compared to our method described above for calculating alpha windows. Absolute parieto-occipital alpha power calculated using a standard alpha window was highly correlated with the individualized window method ($r = .99$, $p < .00001$; Figure S1).

Functional MRI (fMRI)

Acquisition

Imaging data were acquired on a GE 3T MR750 scanner with an 8-channel head coil at the Center for Functional MRI (University of California, San Diego). High-resolution structural images were acquired with a standard FSPGR T1-weighted sequence (TR: 8.108ms, TE: 3.172 ms, flip angle: 8°; FOV 256 mm; 1mm³ resolution; 172 slices). Functional T2*-

weighted images were acquired using a single-shot gradient-recalled, echo-planar imaging pulse sequence (TR: 2000ms; TE: 30 ms; flip angle: 90°; 3.4mm isotropic resolution; FOV: 220mm; matrix: 64 x 64; 42 axial slices). One 6 minute 10 second resting-state scan was obtained consisting of 185 whole-brain volumes. The first five volumes were discarded to account for T1-equilibration effects. Subjects were instructed to fixate on a cross projected onto the middle of a screen, viewed through a mirror in the bore, and to “Let your mind wander, relax, but please stay as still as you can. Do not fall asleep.” Compliance with instructions to remain still and awake was monitored via video recording.

Data Processing

Functional images were processed using Analysis of Functional NeuroImages software (AFNI v17.2.07; Cox, 1996) FMRIB Software Library (FSL; v5.0; Smith et al., 2004), and Freesurfer (Dale et al. 1999, Fischl et al. 1999, Fischl 2012). Images were slice-time corrected and each functional volume was registered to the middle time point of the scan to adjust for motion via rigid-body realignment as implemented in AFNI. Field map correction was applied to minimize distortions due to magnetic field inhomogeneity. The functional images were registered to the anatomical scan via FSL’s FLIRT (Jenkinson & Smith, 2001). Anatomical and functional images were resampled to 3mm isotropic voxels and standardized to the atlas space of the Montreal Neurological Institute (MNI) template using FSL’s nonlinear registration tool (FNIRT). AFNI’s 3dBlurToFWHM was used to smooth functional images to a Gaussian full width at half-maximum (FWHM) of 6 mm. Functional MRI time series were highpass filtered at .008 Hz using a second-order Butterworth filter, which was also applied to the 10 nuisance regressors (see below).

Given the known impact of motion on BOLD correlations (Power et al., 2014), additional measures were taken to correct for motion. The mean signal from ventricles and white matter masks (obtained from Freesurfer segmentation of T1-weighted structural image and eroded by 1 voxel) as well as six motion parameters (obtained from rigid-body realignment) and their first temporal derivatives were regressed from the signal. Residuals from nuisance regression were used for all subsequent functional connectivity analyses. Root mean squared displacement (RMSD), an estimate of head

motion across all time points, was calculated for each participant. Framewise displacement (FD) was calculated as a volume-by-volume measure of motion. Time points with > 0.5 mm FD as well the two subsequent time points were censored. Time series fragments with < 10 consecutive time points remaining after censoring were also excluded. Minimal censoring was performed (ASD mean = 2.8% censored, TD mean = 2.2% censored), and groups did not differ with respect to the number of remaining timepoints (Table 1b). All structural and functional data were visually inspected at every preprocessing stage by at least two blinded reviewers to ensure acceptable data quality.

For ALFF and fractional ALFF (fALFF) analyses, data were processed as above with the exception of highpass filtering and censoring, in order to preserve the full timeseries and range of frequencies. In FC analyses, minimal censoring was necessary in both groups (averages of 2.6% for ASD and 2.2% for TD). Therefore, including these few outlier timepoints for ALFF/fALFF analyses is unlikely to affect findings, which summarize the entire timeseries. Bandpass filtering was applied for ALFF analyses in subsequent analysis steps (described below).

Performing GSR to remove global noise from resting state fMRI time series is controversial and a consensus has not been reached (Liu et al. 2017, Murphy and Fox 2017, Power et al. 2017, Power et al. 2017, Uddin 2017). While the global BOLD signal at least partially reflects physiological artefact (Power et al. 2017) it also contains neural information (Fox et al. 2009, Schölvinck et al. 2010). We matched ASD and TD groups on motion, included only participants with high-quality data, and used white matter and CSF regressors, which have been shown to contain physiological artefact as well, for denoising. GSR was therefore not performed to avoid potentially removing true neuronal signal.

Amplitude of the Low Frequency Function (ALFF)

All ninety-six cortical regions (Table S2) and the thalamus from the Harvard-Oxford Atlas (Bohland et al. 2009) were used as regions of interest (ROIs). This relatively coarse parcellation minimized the computational burden of the current brain-wide analysis. Furthermore, an anatomical parcellation avoids potential confounds related to the greater inter- and intra-individual variability of functional atlases (Salehi et al. 2019), which may be

especially problematic when studying clinical groups. ALFF and fractional ALFF (fALFF) were extracted from each ROI using AFNI's 3dRSFC (Taylor and Saad 2013), with a frequency range of .008-.08 Hz specified for ALFF.

Functional Connectivity

Functional connectivity was assessed between left and right thalamus and all ipsilateral cortical ROIs, given predominantly ipsilateral connectivity between thalamus and cerebral cortex (Jones 2007). Average timecourses were extracted from each ROI using AFNI's 3dmaskave. Pearson correlations were calculated between ipsilateral thalamus and cortical ROIs and then transformed to Fisher's z values.

Analysis Approach

Groups were compared on fMRI measures (i.e., ALFF, fALFF, and thalamocortical FC) at two levels of analysis. 1) In order to reduce the dimensionality of the data while preserving broad regional patterns of interest, multilevel modeling was conducted separately for six mutually exclusive ROI groups in the left and right hemispheres (frontal, limbic, somatomotor, temporal, parietal, occipital; Table S2), which included all 96 cortical ROIs. For example, group differences in ALFF were examined for all left frontal ROIs nested within subjects, all left limbic ROIs nested within subjects, and so on for all six ROI groups in both hemispheres (Figure S2). In other words, for these models each participant had one observation for diagnosis (ASD or TD), and n observations (where n = number of ROIs) for ALFF. Degrees of freedom for each multilevel model were calculated as: (number of participants x number of nested ROIs) – number of model parameters. This approach both reduces the number of comparisons and accounts for non-independence of multiple ROIs within each participant. 2) Following MLM, post-hoc analyses were conducted at the single ROI-level to characterize group differences in finer detail. For ALFF, fALFF, and thalamocortical FC, two-sample t-tests were conducted for each individual cortical ROI and the thalamus, with degrees of freedom adjusted for unequal variances. ROI-level analyses were repeated for an unmedicated subsample of ASD participants and a matched TD group.

Multimodal Analyses

For the 34 individuals described above with both EEG and fMRI data (Table 1c), multimodal analyses were conducted. First, the relationship between absolute EEG alpha power and ALFF, which is considered more comparable to absolute EEG power than fALFF (Luchinger et al. 2012), was examined. Furthermore, ALFF demonstrates better test-retest reliability than fALFF, and is therefore a more appropriate measure for evaluating between-subjects relationships (Zuo et al. 2010). As in fMRI-only analyses, effects of interest were examined with both MLM and at the single ROI-level. MLM was conducted for each of six groups of ROIs (as above) to determine the effect of diagnostic status, alpha power, and their interaction on ALFF. Sex and nonverbal IQ were not well-matched between multimodal groups and were therefore included as covariates. As described above for fMRI MLM, each participant had one observation for each predictor and covariate, and n observations (where n = number of ROIs) for ALFF. At the ROI-level, analogous general linear models were used to examine these effects for each individual cortical ROI and the thalamus.

Finally, the relationship between alpha power and thalamocortical connectivity was explored. As in the multimodal ALFF analysis, MLM was conducted for each ROI group with thalamocortical functional connectivity (Fisher's z) as the dependent variable. General linear models were also run at the ROI-level, as described above.

Multiple Comparison Approach

The analyses described above involve numerous comparisons among cortical ROIs. Traditional approaches to multiple comparison correction rely on conservative adjustments to significance values (i.e., " p -values"), with the goal of reducing Type 1 error or false discovery rate. However, p -values are influenced by data precision, which is closely tied to sample size. Therefore, particularly in smaller samples, inferences based on p -values alone may lead to erroneous conclusions (c.f. Schmidt and Rothman 2014). Alternatively, hierarchical models (i.e., MLM) have been proposed to account for multiple comparisons without the adjustment of p -values (Gelman, Hill, & Yajima, 2012), and have demonstrated specific utility in neuroimaging (Friston et al., 2002; Friston & Penny, 2003). In order to balance between more liberal (i.e., uncorrected p -values for ROI analyses) and conservative approaches (i.e., corrections using MLM), we present results from MLM,

followed up with uncorrected ROI-level comparisons to describe patterns driving MLM findings. Therefore, individual comparisons are best interpreted with caution, and in the context of MLM results.

Results

EEG Analyses

In the full sample with resting-state EEG data, the ASD group showed reduced absolute ($t(60.41) = 2.74, p = .008$) and relative ($t(73.42) = 3.83, p < .001$) power in the alpha frequency band (Figure 1). Groups did not differ with respect to alpha peak frequency ($t(58.40) = -0.23, p = .82$). In a supplemental analysis of only unmedicated ASD participants and a matched TD subgroup ($n = 17$ per group), similar differences were found in both absolute ($t(27.17) = -2.22, p = .04$) and relative alpha power ($t(31.30) = -2.39, p = .02$; Figure S3), and there were no significant group differences for alpha peak frequency ($t(30.13) = 1.24, p = .23$).

Functional MRI Analyses

MLM suggested increased fALFF (ASD > TD) in right temporal regions ($t(1843) = 2.45, p = .01$; Table S3). In ROI-level analyses, ALFF was increased in ASDs in both the anterior ($t(108.50) = 2.58, p = .01$) and posterior ($t(116.52) = 2.00, p = .048$) segments of the right middle temporal gyrus, and fALFF was increased in ASDs in 12 temporal and occipital ROIs spanning both hemispheres (p range = $[\.002, .046]$; Figure 2A, Table S4). Finally, at the ROI-level there were no group differences in ALFF or fALFF in the thalamus (both $p > .70$).

With respect to thalamocortical FC, MLM revealed ipsilateral overconnectivity (ASD > TD) involving bilateral frontal, somatomotor, and temporal, as well as left limbic regions (p range = $[\.002, .03]$, Table S3). ROI-level results were consistent and are presented in Figure 2A and Table S4. Supplemental analyses of unmedicated ASD participants and a matched TD subsample ($n = 37$ per group) yielded similar results for ALFF, fALFF, and FC to those reported in the full sample (Figure S4).

Multimodal Analyses

Alpha Power and ALFF

MLM showed multiple alpha by diagnosis interactions with respect to ALFF (i.e., the alpha-ALFF relationship differed between groups) in bilateral frontal, limbic, and somatomotor ROI groups, with consistently less positive relationships between ALFF and alpha power in the ASD compared to the TD group (p range = [.01, .04]; Table S5). Furthermore, MLM combining all 96 cortical ROIs in the ASD group alone found that across the whole brain, there was an interaction between ADOS total score and alpha power ($t(1628) = -2.44$, $p = .01$), such that greater ASD symptom severity predicted an overall less positive relationship between alpha power and ALFF. Finally, within the ASD group there was no effect of medication on the overall relationship between alpha power and ALFF in whole-brain MLM ($p = .90$).

At the ROI-level, thalamic ALFF was not predicted by absolute alpha power, diagnosis, or their interaction (all $p > .09$). Findings for cortical ROIs were consistent with MLM analysis, suggesting that alpha-ALFF relationships differed between groups in 15 frontal, limbic, somatomotor, and temporal ROIs (Figure 2B, Figure S5, Table 2). Follow-up Pearson correlations determined that across all cortical ROIs, alpha power and ALFF were more positively related in the TD group (mean $r = .40$, range = [.11, .70]) than in the ASD group (mean $r = -.18$, range = [-.61, .17]). One-sample t-tests of alpha-ALFF correlations (transformed to Fisher's z) for each ROI corroborated that this relationship was significantly greater than zero in the TD group ($t(95) = 22.15$, $p < .0001$), but significantly less than zero in the ASD group ($t(95) = -10.90$, $p < .0001$).

Alpha Power and Thalamocortical FC

There was no effect of alpha, diagnosis, or their interaction on thalamocortical connectivity in MLM (all $p > .11$; Table S5). One-sample t-tests indicated that overall, the correlation between EEG alpha and thalamocortical FC was significantly less than zero in both the ASD ($t(95) = -8.95$, $p < .0001$) and TD groups ($t(95) = -3.62$, $p < .001$). At the ROI-level, the ASD group showed a more positive relationship between alpha power and

thalamocortical FC than the TD group for the right angular and supramarginal gyri, whereas the opposite effect of group was observed in the occipital pole (p range = [.003, .03]; Table 2).

Discussion

Our study replicates two commonly reported findings from the unimodal EEG and fMRI literatures, showing reduced alpha power as well as predominantly increased thalamocortical connectivity in children and adolescents with ASDs. Although no robust group differences were detected for ALFF, findings suggest spontaneous BOLD fluctuations in right temporal lobe may be increased in ASDs. Multimodal analyses identified group differences in the relationship between EEG alpha power and ALFF, but not between alpha power and thalamocortical FC.

Unimodal Group Differences

Reduced EEG alpha in ASDs

In line with previous research (Murias et al. 2007, Keehn et al. 2017) our EEG sample showed atypically reduced posterior (i.e., occipital or parietal) resting state alpha power in children and adolescents with ASDs. Although the resting alpha rhythm is most prominent at posterior electrodes, reduced alpha power in ASDs has also been reported more broadly in frontal and temporal regions (for review, see Wang et al. 2013). The resting alpha rhythm is inversely associated with autonomic arousal (i.e., electrodermal activity) in typically developing children (Barry et al. 2004), which is thought to be coordinated largely by inhibitory GABAergic interneurons (Jensen and Mazaheri 2010). In ASDs, an imbalance between excitatory and inhibitory neural activity has been proposed (Rubenstein and Merzenich 2003, Nelson and Valakh 2015), which may lead to such changes in autonomic activity. This is supported by evidence of tonic hyperarousal (Palkovitz and Wiesenfeld 1980) as well as histological (Oblak et al. 2010, Hashemi et al. 2017) and magnetic resonance spectroscopy reports (Gaetz et al. 2014, Puts et al. 2017) of reduced GABA in this population.

Increased thalamocortical connectivity in ASDs

Previous findings with respect to thalamocortical FC in ASDs have been only partially consistent. Nair et al. (2015), who included a smaller sample partly overlapping with that of the current study, reported primarily reduced thalamocortical FC with frontal, parietal, and occipital regions and increased FC with auditory, primary motor, and limbic areas. These slightly different findings may be attributed to methodological differences. For example, the focus on functional differences *within* the thalamus through voxelwise analyses in Nair et al. (2015), contrasts with focus on overall thalamic connectivity with each cortical ROI in the present study.

Similarly to Nair et al. (2015), Cerliani et al. (2015) reported overconnectivity between thalamus and primary sensory and motor networks (including somatosensory, motor, visual, and auditory regions) identified through independent component analysis in a larger sample of children and adults (ages 7-50; 166 ASD, 193 TD) from the Autism Brain Imaging Data Exchange (ABIDE) database, however, they did not find any evidence of thalamocortical underconnectivity. Another study using a large ABIDE sample (ages 6-40; n=228 per group) described overconnectivity between thalamus and primary sensory cortices (including somatosensory, motor, and temporal regions) as well as prefrontal cortex (Woodward et al. 2017). Furthermore, they reported greatest overconnectivity in older adolescents (ages 13-18) compared to other age groups. These findings are consistent with results from the current study, which also found exclusive overconnectivity with frontal, temporal, somatomotor, and limbic ROIs in children and adolescents.

Regionally Increased BOLD activity in ASDs

The results of the current study support increased BOLD activity (i.e., ALFF, fALFF) in bilateral (right more than left) temporal and occipital regions; no evidence of decreased ALFF or fALFF was found. These findings are only partly consistent with extremely limited previous research examining ALFF and fALFF in ASDs. In a multi-site study, Supekar et al. (2013) reported broadly increased ALFF across the brain in ASDs in multiple independent cohorts of children. In a large ABIDE sample, increased fALFF was found in right temporal regions (as in the current study), as well as in right dorsal superior frontal cortex (Di

Martino et al. 2014). However, this same study and another (Itahashi et al. 2015) reported reduced fALFF in left and right occipital regions in ASDs. This is opposite the findings from the current study, which were exclusively positive (i.e., ASD > TD) for both temporal and occipital regions.

EEG-fMRI Associations Differ Between Groups

EEG Alpha and ALFF

Relationships between EEG alpha power and fMRI measures were surprising and seemingly counterintuitive, in light of the well-established inverse relationship between concurrent (i.e., simultaneously acquired) EEG alpha and cortical BOLD activity in TD adults. However, simultaneous alpha and BOLD timeseries are distinct from overall alpha power and ALFF, which were measured in the current study. The former describes moment-to-moment fluctuations, but the latter provide summary measures of alpha and BOLD magnitude across an entire recording session. In the current study, alpha power had an overall *positive* relationship with spontaneous BOLD activity (ALFF) in TD adolescents, but a weakly negative relationship with ALFF in those with ASDs. This difference was driven mainly by frontal, limbic, and somatomotor regions. Furthermore, a more negative alpha-ALFF relationship across the entire brain was associated with greater ASD symptom severity. The underlying neural basis of this relationship remains unclear but may relate to differences in inhibitory GABAergic activity, as described earlier. Importantly, GABA is thought to mediate thalamocortical regulation of the alpha rhythm (Hughes and Crunelli 2005, Lorincz et al. 2009, Lozano-Soldevilla et al. 2014). Therefore, impaired GABAergic signaling in ASDs could conceivably disrupt modulation of alpha rhythms by thalamic and cortical activity, leading to an atypically weak relationship between alpha and cortical BOLD magnitudes in ASDs.

EEG Alpha and Thalamocortical FC

Thalamocortical FC and EEG alpha power showed overall weakly negative associations in both ASD and TD groups across the brain. This diverges from findings described above for ALFF; while the magnitude of BOLD activity appears to be dissociated from alpha power in ASDs, coordination between thalamus and cortex shows a comparatively normal

relationship with alpha power in the ASD group. This negative alpha-FC relationship across groups in our multimodal sample may be considered in relation to unimodal results in our larger EEG and fMRI samples. Specifically, the ASD samples showed reduced alpha power in EEG analyses, but widespread overconnectivity between thalamus and frontal, limbic, somatomotor, and temporal ROIs in fcMRI analyses. The overall negative relation between alpha and thalamocortical FC detected in both ASD and TD subsamples with multimodal data suggests that the two findings in the larger unimodal samples may be related, implying that children with ASDs with most severely reduced alpha power will also tend to show heavier overconnectivity between thalamus and cerebral cortex.

Limitations and Future Directions

The current study included a limited subsample of participants with high-quality data in both EEG and fMRI modalities. Furthermore, only high-functioning individuals with ASDs could be included, who may not represent the full autism spectrum. Future studies with larger samples representing a broader range of ASD symptom severity may help to clarify some of the patterns suggested by the current study.

Another important consideration is the distinction between multimodal relationships within versus between individuals. Past research using simultaneous recordings has examined concurrent fluctuations in EEG and fMRI within typically developing adults, or “state-level” associations. Separately acquired data cannot answer this question, but they can speak to how these signals are related between individuals, at the “trait-level.” For example, it has been established that within individuals (state-level), moment-to-moment increases in EEG alpha power are associated with concurrent decreases in cortical (but not thalamic) BOLD (Goldman et al. 2002, Laufs et al. 2003, Olbrich et al. 2009, Bridwell et al. 2013). However, the present study suggests a seemingly opposite relationship *between* typical developing individuals (trait-level), such that those showing higher overall alpha power also show greater magnitude of spontaneous BOLD fluctuations. These trait-level associations are an important bridge between fMRI and EEG research in ASDs. Group differences reported by unimodal studies suggest that there are meaningful, interindividual differences between ASD and TD groups. Therefore, a clear understanding of normative interindividual relationships between multimodal measures will provide a common context

for interpreting past EEG and fMRI findings. Future research may further explore these important questions with simultaneous EEG-fMRI when possible, and by conducting both within-subjects analysis of temporal dynamics as well as between-subjects analysis of multimodal relationships.

Conclusion

This is the first known study to characterize relationships between resting state EEG and fMRI measures in ASDs. Reduced alpha power and broadly increased thalamocortical connectivity were found in ASDs relative to TD individuals. Results also suggest a positive relationship between EEG alpha power and cortical BOLD activity in typical development, which was not observed in ASDs. These findings raise questions for future research about potential abnormalities in thalamocortical regulation of the alpha rhythm in this disorder.

Acknowledgments

The authors would like to acknowledge Marissa Westerfield and Wen-Hsuan Chan for their contributions to the preprocessing EEG data, and Christopher Fong for preprocessing of fMRI data. This work was funded by the National Institutes of Health R01 MH081023 (RAM), R21 MH102578 (RAM, TTL), R01 MH101173 (RAM), R21 MH096582 (JT), National Institute of Neurological Disorders and Stroke Center Grant 2P50NS22343 (JT), and National Science Foundation Graduate Research Fellowship 1321850 (LEM).

Author Disclosure Statement

No competing financial interests exist.

References

- Allen, E. A., E. Damaraju, T. Eichele, L. Wu, V. D. Calhoun. 2018. EEG Signatures of Dynamic Functional Network Connectivity States. *Brain Topogr* 31(1): 101-116.
- American Psychiatric Association (2013). *Diagnostic and statistical manual of mental disorders : DSM-5* Arlington, VA, American Psychiatric Association: 947.
- Baio, J., L. Wiggins, D. L. Christensen, M. J. Maenner, J. Daniels, Z. Warren, et al. 2018. Prevalence of Autism Spectrum Disorder Among Children Aged 8 Years - Autism and Developmental Disabilities Monitoring Network, 11 Sites, United States, 2014. *MMWR Surveill Summ* 67(6): 1-23.
- Barry, R. J., A. R. Clarke, R. McCarthy, M. Selikowitz, J. A. Rushby, E. Ploskova. 2004. EEG differences in children as a function of resting-state arousal level. *Clin Neurophysiol* 115(2): 402-408.
- Bohland, J. W., H. Bokil, C. B. Allen, P. P. Mitra. 2009. The brain atlas concordance problem: quantitative comparison of anatomical parcellations. *PLoS One* 4(9): e7200.
- Bridwell, D. A., L. Wu, T. Eichele, V. D. Calhoun. 2013. The spatospectral characterization of brain networks: fusing concurrent EEG spectra and fMRI maps. *Neuroimage* 69: 101-111.
- Britton, J. W., L. C. Frey, J. L. Hopp, P. Korb, M. Z. Koubeissi, W. E. Lievens, et al. 2016. *Electroencephalography (EEG): An Introductory Text and Atlas of Normal and Abnormal Findings in Adults, Children, and Infants*. Chicago, IL: American Epilepsy Society.
- Cerliani, L., M. Mennes, R. M. Thomas, A. Di Martino, M. Thioux, C. Keysers. 2015. Increased Functional Connectivity Between Subcortical and Cortical Resting-State Networks in Autism Spectrum Disorder. *JAMA Psychiatry* 72(8): 767-777.
- Chan, A. S., S. L. Sze, M. C. Cheung. 2007. Quantitative electroencephalographic profiles for children with autistic spectrum disorder. *Neuropsychology* 21(1): 74-81.

Cragg, L., N. Kovacevic, A. R. McIntosh, C. Poulsen, K. Martinu, G. Leonard, T. Paus. 2011. Maturation of EEG power spectra in early adolescence: a longitudinal study. *Dev Sci* 14(5): 935-943.

Dale, A. M., B. Fischl, M. I. Sereno. 1999. Cortical surface-based analysis. I. Segmentation and surface reconstruction. *Neuroimage* 9(2): 179-194.

Dawson, G., L. G. Klinger, H. Panagiotides, A. Lewy, P. Castelloe. 1995. Subgroups of autistic children based on social behavior display distinct patterns of brain activity. *J Abnorm Child Psychol* 23(5): 569-583.

de Munck, J. C., S. I. Goncalves, L. Huijboom, J. P. Kuijer, P. J. Pouwels, R. M. Heethaar, F. H. Lopes da Silva. 2007. The hemodynamic response of the alpha rhythm: an EEG/fMRI study. *Neuroimage* 35(3): 1142-1151.

Delorme, A., S. Makeig. 2004. EEGLAB: an open source toolbox for analysis of single-trial EEG dynamics including independent component analysis. *J Neurosci Methods* 134(1): 9-21.

Di Martino, A., C. G. Yan, Q. Li, E. Denio, F. X. Castellanos, K. Alaerts, et al. 2014. The autism brain imaging data exchange: towards a large-scale evaluation of the intrinsic brain architecture in autism. *Mol Psychiatry* 19(6): 659-667.

Dickinson, A., C. DiStefano, D. Senturk, S. S. Jeste. 2018. Peak alpha frequency is a neural marker of cognitive function across the autism spectrum. *Eur J Neurosci* 47(6): 643-651.

Edgar, J. C., K. Heiken, Y. H. Chen, J. D. Herrington, V. Chow, S. Liu, et al. 2015. Resting-state alpha in autism spectrum disorder and alpha associations with thalamic volume. *J Autism Dev Disord* 45(3): 795-804.

Fischl, B. 2012. FreeSurfer. *Neuroimage* 62(2): 774-781.

Fischl, B., M. I. Sereno, A. M. Dale. 1999. Cortical surface-based analysis. II: Inflation, flattening, and a surface-based coordinate system. *Neuroimage* 9(2): 195-207.

Fox, M. D., D. Zhang, A. Z. Snyder, M. E. Raichle. 2009. The global signal and observed anticorrelated resting state brain networks. *J Neurophysiol* 101(6): 3270-3283.

Gaetz, W., L. Bloy, D. J. Wang, R. G. Port, L. Blaskey, S. E. Levy, T. P. Roberts. 2014. GABA estimation in the brains of children on the autism spectrum: measurement precision and regional cortical variation. *Neuroimage* 86: 1-9.

Goldman, R. I., J. M. Stern, J. Engel, Jr., M. S. Cohen. 2002. Simultaneous EEG and fMRI of the alpha rhythm. *Neuroreport* 13(18): 2487-2492.

Gotham, K., S. Risi, A. Pickles, C. Lord. 2007. The Autism Diagnostic Observation Schedule: revised algorithms for improved diagnostic validity. *J Autism Dev Disord* 37(4): 613-627.

Haegens, S., H. Cousijn, G. Wallis, P. J. Harrison, A. C. Nobre. 2014. Inter- and intra-individual variability in alpha peak frequency. *Neuroimage* 92: 46-55.

Hames, E. C., B. Murphy, R. Rajmohan, R. C. Anderson, M. Baker, S. Zupancic, et al. 2016. Visual, Auditory, and Cross Modal Sensory Processing in Adults with Autism: An EEG Power and BOLD fMRI Investigation. *Front Hum Neurosci* 10: 167.

Hashemi, E., J. Ariza, H. Rogers, S. C. Noctor, V. Martinez-Cerdeno. 2017. The Number of Parvalbumin-Expressing Interneurons Is Decreased in the Prefrontal Cortex in Autism. *Cereb Cortex* 27(3): 1931-1943.

Hillman, E. M. 2014. Coupling mechanism and significance of the BOLD signal: a status report. *Annu Rev Neurosci* 37: 161-181.

Hughes, S. W., V. Crunelli. 2005. Thalamic mechanisms of EEG alpha rhythms and their pathological implications. *Neuroscientist* 11(4): 357-372.

Hull, J. V., Z. J. Jacokes, C. M. Torgerson, A. Irimia, J. D. Van Horn. 2016. Resting-State Functional Connectivity in Autism Spectrum Disorders: A Review. *Front Psychiatry* 7: 205.

Itahashi, T., T. Yamada, H. Watanabe, M. Nakamura, H. Ohta, C. Kanai, et al. 2015. Alterations of local spontaneous brain activity and connectivity in adults with high-functioning autism spectrum disorder. *Mol Autism* 6: 30.

Jensen, O., A. Mazaheri. 2010. Shaping functional architecture by oscillatory alpha activity: gating by inhibition. *Front Hum Neurosci* 4: 186.

Jochaut, D., K. Lehongre, A. Saitovitch, A. D. Devauchelle, I. Ollasagasti, N. Chabane, et al. 2015. Atypical coordination of cortical oscillations in response to speech in autism. *Front Hum Neurosci* 9: 171.

Jones, E. G. 2007. *The Thalamus*: Cambridge University Press. p. 142-146

Jung, T. P., S. Makeig, C. Humphries, T. W. Lee, M. J. McKeown, V. Iragui, T. J. Sejnowski. 2000. Removing electroencephalographic artifacts by blind source separation. *Psychophysiology* 37(2): 163-178.

Jung, T. P., S. Makeig, M. Westerfield, J. Townsend, E. Courchesne, T. J. Sejnowski. 2000. Removal of eye activity artifacts from visual event-related potentials in normal and clinical subjects. *Clin Neurophysiol* 111(10): 1745-1758.

Keehn, B., M. Westerfield, R. A. Muller, J. Townsend. 2017. Autism, Attention, and Alpha Oscillations: An Electrophysiological Study of Attentional Capture. *Biol Psychiatry Cogn Neurosci Neuroimaging* 2(6): 528-536.

Klimesch, W. 1999. EEG alpha and theta oscillations reflect cognitive and memory performance: a review and analysis. *Brain Res Brain Res Rev* 29(2-3): 169-195.

Laufs, H., A. Kleinschmidt, A. Beyerle, E. Eger, A. Salek-Haddadi, C. Preibisch, K. Krakow. 2003. EEG-correlated fMRI of human alpha activity. *Neuroimage* 19(4): 1463-1476.

Liu, T. T., A. Nalci, M. Falahpour. 2017. The global signal in fMRI: Nuisance or Information? *Neuroimage* 150: 213-229.

Lord, C., S. Risi, L. Lambrecht, E. H. Cook, Jr., B. L. Leventhal, P. C. DiLavore, et al. 2000. The autism diagnostic observation schedule-generic: a standard measure of social and communication deficits associated with the spectrum of autism. *J Autism Dev Disord* 30(3): 205-223.

Lorincz, M. L., K. A. Kekesi, G. Juhasz, V. Crunelli, S. W. Hughes. 2009. Temporal framing of thalamic relay-mode firing by phasic inhibition during the alpha rhythm. *Neuron* 63(5): 683-696.

Lozano-Soldevilla, D., N. ter Huurne, R. Cools, O. Jensen. 2014. GABAergic modulation of visual gamma and alpha oscillations and its consequences for working memory performance. *Curr Biol* 24(24): 2878-2887.

Luchinger, R., L. Michels, E. Martin, D. Brandeis. 2012. Brain state regulation during normal development: Intrinsic activity fluctuations in simultaneous EEG-fMRI. *Neuroimage* 60(2): 1426-1439.

Mash, L. E., M. A. Reiter, A. C. Linke, J. Townsend, R. A. Müller. 2018. Multimodal approaches to functional connectivity in autism spectrum disorders: An integrative perspective. *Dev Neurobiol* 78(5): 456-473.

Miskovic, V., X. Ma, C. A. Chou, M. Fan, M. Owens, H. Sayama, B. E. Gibb. 2015. Developmental changes in spontaneous electrocortical activity and network organization from early to late childhood. *Neuroimage* 118: 237-247.

Murias, M., S. J. Webb, J. Greenson, G. Dawson. 2007. Resting state cortical connectivity reflected in EEG coherence in individuals with autism. *Biol Psychiatry* 62(3): 270-273.

Murphy, K., M. D. Fox. 2017. Towards a consensus regarding global signal regression for resting state functional connectivity MRI. *Neuroimage* 154: 169-173.

Nair, A., R. A. Carper, A. E. Abbott, C. P. Chen, S. Solders, S. Nakutin, et al. 2015. Regional specificity of aberrant thalamocortical connectivity in autism. *Hum Brain Mapp* 36(11): 4497-4511.

Nelson, S. B., V. Valakh. 2015. Excitatory/Inhibitory Balance and Circuit Homeostasis in Autism Spectrum Disorders. *Neuron* 87(4): 684-698.

Niedermeyer, E., D. L. Schomer, F. H. Lopes da Silva. 2011. *Niedermeyer's electroencephalography : basic principles, clinical applications, and related fields*. Philadelphia: Wolters Kluwer Health/Lippincott Williams & Wilkins.p.

O'Reilly, C., J. D. Lewis, M. Elsabbagh. 2017. Is functional brain connectivity atypical in autism? A systematic review of EEG and MEG studies. *PLoS One* 12(5): e0175870.

Oblak, A. L., T. T. Gibbs, G. J. Blatt. 2010. Decreased GABAB receptors in the cingulate cortex and fusiform gyrus in Autism. *Journal of Neurochemistry* 114(5): 1414-1423.

Olbrich, S., C. Mulert, S. Karch, M. Trenner, G. Leicht, O. Pogarell, U. Hegerl. 2009. EEG-vigilance and BOLD effect during simultaneous EEG/fMRI measurement. *Neuroimage* 45(2): 319-332.

Oostenveld, R., P. Fries, E. Maris, J. M. Schoffelen. 2011. FieldTrip: Open source software for advanced analysis of MEG, EEG, and invasive electrophysiological data. *Comput Intell Neurosci* 2011: 156869.

Palkovitz, R. J., A. R. Wiesenfeld. 1980. Differential autonomic responses of autistic and normal children. *J Autism Dev Disord* 10(3): 347-360.

Power, J. D., T. O. Laumann, M. Plitt, A. Martin, S. E. Petersen. 2017. On Global fMRI Signals and Simulations. *Trends Cogn Sci* 21(12): 911-913.

Power, J. D., M. Plitt, T. O. Laumann, A. Martin. 2017. Sources and implications of whole-brain fMRI signals in humans. *Neuroimage* 146: 609-625.

Puts, N. A. J., E. L. Wodka, A. D. Harris, D. Crocetti, M. Tommerdahl, S. H. Mostofsky, R. A. E. Edden. 2017. Reduced GABA and altered somatosensory function in children with autism spectrum disorder. *Autism Res* 10(4): 608-619.

Rubenstein, J. L., M. M. Merzenich. 2003. Model of autism: increased ratio of excitation/inhibition in key neural systems. *Genes Brain Behav* 2(5): 255-267.

Salehi, M., A. S. Greene, A. Karbasi, X. Shen, D. Scheinost, R. T. Constable. 2019. There is no single functional atlas even for a single individual: Parcellation of the human brain is state dependent. *bioRxiv*: 431833.

Scheeringa, R., K. M. Petersson, A. Kleinschmidt, O. Jensen, M. C. Bastiaansen. 2012. EEG alpha power modulation of fMRI resting-state connectivity. *Brain Connect* 2(5): 254-264.

Schmidt, M., K. J. Rothman. 2014. Mistaken inference caused by reliance on and misinterpretation of a significance test. *International Journal of Cardiology* 177(3): 1089-1090.

Schölvinck, M. L., A. Maier, F. Q. Ye, J. H. Duyn, D. A. Leopold. 2010. Neural basis of global resting-state fMRI activity. *Proc Natl Acad Sci U S A* 107(22): 10238-10243.

Schuetze, M., M. T. Park, I. Y. Cho, F. P. MacMaster, M. M. Chakravarty, S. L. Bray. 2016. Morphological Alterations in the Thalamus, Striatum, and Pallidum in Autism Spectrum Disorder. *Neuropsychopharmacology* 41(11): 2627-2637.

Sheikhani, A., H. Behnam, M. R. Mohammadi, M. Noroozian, M. Mohammadi. 2012. Detection of abnormalities for diagnosing of children with autism disorders using of quantitative electroencephalography analysis. *J Med Syst* 36(2): 957-963.

Supek, S., C. J. Aine (2014). Magnetoencephalography : from signals to dynamic cortical networks: 1 online resource.

Supekar, K., L. Q. Uddin, A. Khouzam, J. Phillips, W. D. Gaillard, L. E. Kenworthy, et al. 2013. Brain hyperconnectivity in children with autism and its links to social deficits. *Cell Rep* 5(3): 738-747.

Taylor, P. A., Z. S. Saad. 2013. FATCAT: (an efficient) Functional and Tractographic Connectivity Analysis Toolbox. *Brain Connect* 3(5): 523-535.

Tierney, A. L., L. Gabard-Durnam, V. Vogel-Farley, H. Tager-Flusberg, C. A. Nelson. 2012. Developmental trajectories of resting EEG power: an endophenotype of autism spectrum disorder. *PLoS One* 7(6): e39127.

Uddin, L. Q. 2017. Mixed Signals: On Separating Brain Signal from Noise. *Trends Cogn Sci* 21(6): 405-406.

Wang, J., J. Barstein, L. E. Ethridge, M. W. Mosconi, Y. Takarae, J. A. Sweeney. 2013. Resting state EEG abnormalities in autism spectrum disorders. *J Neurodev Disord* 5(1): 24.

Woodward, N. D., M. Giraldo-Chica, B. Rogers, C. J. Cascio. 2017. Thalamocortical dysconnectivity in autism spectrum disorder: An analysis of the Autism Brain Imaging Data Exchange. *Biol Psychiatry Cogn Neurosci Neuroimaging* 2(1): 76-84.

Xia, M., J. Wang, Y. He. 2013. BrainNet Viewer: a network visualization tool for human brain connectomics. *PLoS One* 8(7): e68910.

Zang, Y. F., Y. He, C. Z. Zhu, Q. J. Cao, M. Q. Sui, M. Liang, et al. 2007. Altered baseline brain activity in children with ADHD revealed by resting-state functional MRI. *Brain Dev* 29(2): 83-91.

Zou, Q. H., C. Z. Zhu, Y. Yang, X. N. Zuo, X. Y. Long, Q. J. Cao, et al. 2008. An improved approach to detection of amplitude of low-frequency fluctuation (ALFF) for resting-state fMRI: fractional ALFF. *J Neurosci Methods* 172(1): 137-141.

Zuo, X. N., A. Di Martino, C. Kelly, Z. E. Shehzad, D. G. Gee, D. F. Klein, et al. 2010. The oscillating brain: complex and reliable. *Neuroimage* 49(2): 1432-1445.

Figure Legends

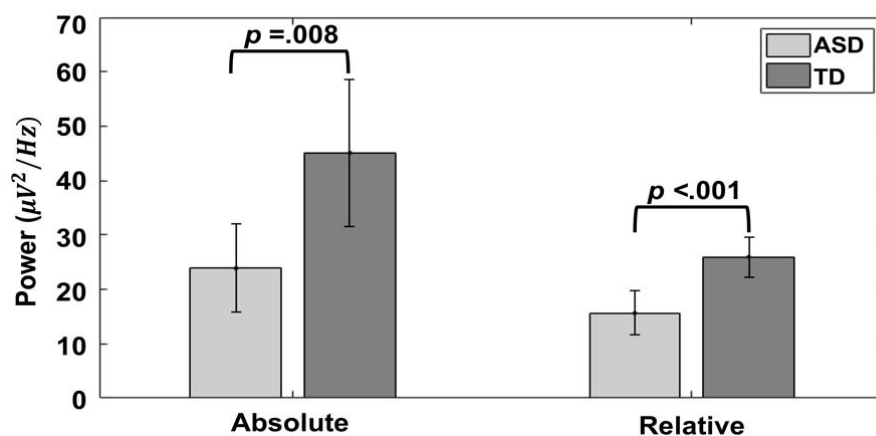


Figure 1. Group Differences in EEG Alpha Power. Bars show absolute and relative alpha power averaged across participants in each group. Both absolute and relative alpha power are smaller in the ASD group than the TD group.

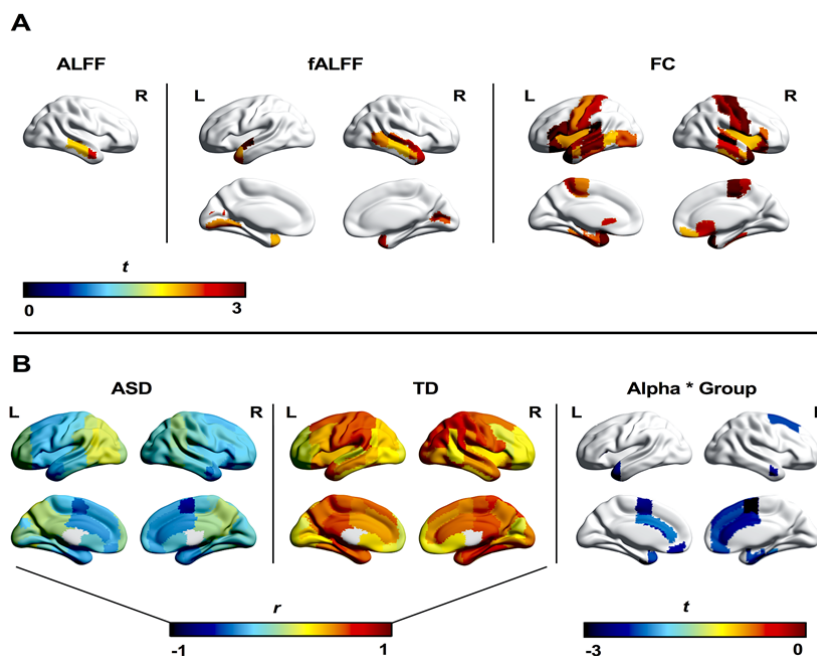


Figure 2. fMRI and Multimodal Group Differences. Panel A: ROIs showing significant group differences ($p < .05$, uncorr.) in ALFF (left), fALFF (middle), and thalamocortical FC (right) are depicted. Colors represent t-scores (positive indicates ASD > TD). Panel B: Pearson correlations (colors represent r) between EEG alpha power and ALFF are depicted for each cortical ROI in the ASD group (left) and the TD group (middle). Alpha-ALFF relationships are generally negative in the ASD group, but positive in the TD group. ROIs with significant group differences in the alpha-ALFF relationship (i.e., alpha by group interaction; $p < .05$, uncorr.) are shown (right). Colors represent t-scores (negative indicates a less positive alpha-ALFF association in ASD relative to TD). Figures were visualized with the BrainNet Viewer (Xia et al. 2013, <http://www.nitrc.org/projects/bnv>)

Table 1a. EEG Sample Characteristics

	ASD (<i>n</i> = 38)	TD (<i>n</i> = 38)	Statistic	<i>p</i>
Sex	32 male	29 male	$\chi^2(1) = 0.75$.39
Handedness	35 right	32 right	$\chi^2(1) = 1.13$.29
			$t(74) = -$	
Age	12.6 (2.4)	13.0 (2.8)	0.57	.57
	[7.1 – 17.1]	[7.1 – 18.0]		
Usable EEG (min)	4.9 (.96)	5.2 (.73)	$t(74) = -1.83$.07
	[2.2 – 6.0]	[2.9 – 6.0]		
			$t(74) = -$	
VIQ	105 (18)	108 (11)	0.86	.39
	[72 – 147]	[83 – 126]		
			$t(74) = -$	
NVIQ	104 (18)	107 (12)	0.61	.54
	[64 – 140]	[77 – 129]		
ADOS SC	10 (4)			
	[1 – 19]			
ADOS RRB	4 (4)			
	[0 – 19]			
ADOS Total	14 (4)			
	[8 – 23]			

This paper has been peer-reviewed and accepted for publication, but has yet to undergo copyediting and proof correction. The final published version may differ from this proof.

Table 1b. fMRI Sample Characteristics

	ASD (<i>n</i> = 66)	TD (<i>n</i> = 57)	Statistic	<i>p</i>
Sex	54 male	45 male	$\chi^2(1) = 0.16$.69
Handedness	58 right	49 right	$\chi^2(1) = 0.10$.75
Age	13.4 (2.6) [8.0-18.0]	13.1 (2.8) [6.9-17.6]	$t(121) = 0.53$.60
Usable fMRI (timepoints)	175 (7) [144 – 180]	176 (7) [145 – 180]	$t(121) = -0.48$.63
RMSD	0.08 (0.04) [0.02 – 0.19]	0.07 (0.04) [0.02 – 0.17]	$t(121) = 0.36$ $t(121) = -$.72
VIQ	101 (17) [67 - 147]	107 (11) [73 - 127]	2.19	.03
NVIQ	105 (17) [53 – 140]	106 (13) [62 - 137]	$t(121) = -0.58$.56
ADOS SC	12 (4) [6 – 22]			
ADOS RRB	2 (2) [0 – 7]			
ADOS Total	14 (4) [7 – 24]			

This paper has been peer-reviewed and accepted for publication, but has yet to undergo copyediting and proof correction. The final published version may differ from this proof.

Brain Connectivity
Atypical relationships between spontaneous EEG and fMRI activity in autism (DOI: 10.1089/brain.2019.0693)

Table 1c. EEG-fMRI Sample Characteristics

	ASD (<i>n</i> = 17)	TD (<i>n</i> = 17)	Statistic	<i>p</i>
			$\chi^2(1) =$	
Sex	16 male	13 male	2.11	.15
			$\chi^2(1) =$	
Handedness	15 right	13 right	0.81	.37
			$t(32) = -$	
Age	14.3 (1.5) [12.7 – 17.1]	14.5 (1.4) [12.4 – 16.8]	0.43	.67
			$t(32) =$	
Usable EEG (min)	5.3 (0.59) [3.9– 6.0]	5.2 (0.72) [2.9 – 5.9]	0.07	.94
			$t(32) = -$	
Usable fMRI (timepoints)	176 (7) [153 – 180]	177 (5) [165 – 180]	0.53	.60
			$t(32) = -$	
RMSD	0.07 (0.04) [0.02 – 0.15]	0.07 (0.04) [0.03 – 0.16]	0.17	.87
			$t(32) =$	
VIQ	116 (13) [88– 147]	107 (10) [87– 126]	2.32	.03
			$t(32) =$	
NVIQ	116 (11) [100 – 140]	110 (12) [86 – 129]	1.67	.11
ADOS SC	10 (3) [7 – 19]			
ADOS RRB	2 (1)			

This paper has been peer-reviewed and accepted for publication, but has yet to undergo copyediting and proof correction. The final published version may differ from this proof.

	[0 – 4]
ADOS Total	12 (4)
	[8 – 23]

^aValues are presented as mean (SD), [range].

^bVIQ = Verbal IQ; NVIQ = Nonverbal IQ; FSIQ = Full Scale IQ; ADOS = Autism Diagnostic Observation Schedule; SC = Social Communication; RRB = Restricted/Repetitive Behavior; RMSD = Root Mean Squared Displacement

Table 2. ROI-level EEG-fMRI Findings

Outcome	Region	df	Alpha*Group	<i>p</i>
			(<i>t</i>)	
ALFF	L Frontal Medial Cortex	28	-2.40	.02
	L Frontal Operculum Cortex	28	-3.17	.004
	L Cingulate Gyrus (anterior)	28	-2.16	.04
	L Supplementary Motor Cortex	28	-2.53	.02
	L Temporal Fusiform Cortex (anterior)	28	-2.94	.007
	L Temporal Pole	28	-2.28	.03
	R Frontal Medial Cortex	28	-2.26	.03
	R Superior Frontal Gyrus	28	-2.32	.03
	R Cingulate Gyrus (anterior)	28	-2.38	.02
	R Paracingulate Gyrus	28	-2.24	.03
	R Parahippocampal Gyrus (anterior)	28	-2.28	.03
	R Supplementary Motor Cortex	28	-3.49	.002
	R Middle Temporal Gyrus (anterior)	28	-2.50	.02
	R Temporal Fusiform Cortex (anterior)	28	-2.30	.03
	R Temporal Fusiform Cortex (posterior)	28	-2.09	.046
Thalamocortical FC	R Angular Gyrus	28	3.21	.003
	R Supramarginal Gyrus (posterior)	28	2.33	.03
	R Occipital Pole	28	-2.52	.02

^a ROIs with group differences ($p < .05$, uncorr) are shown.

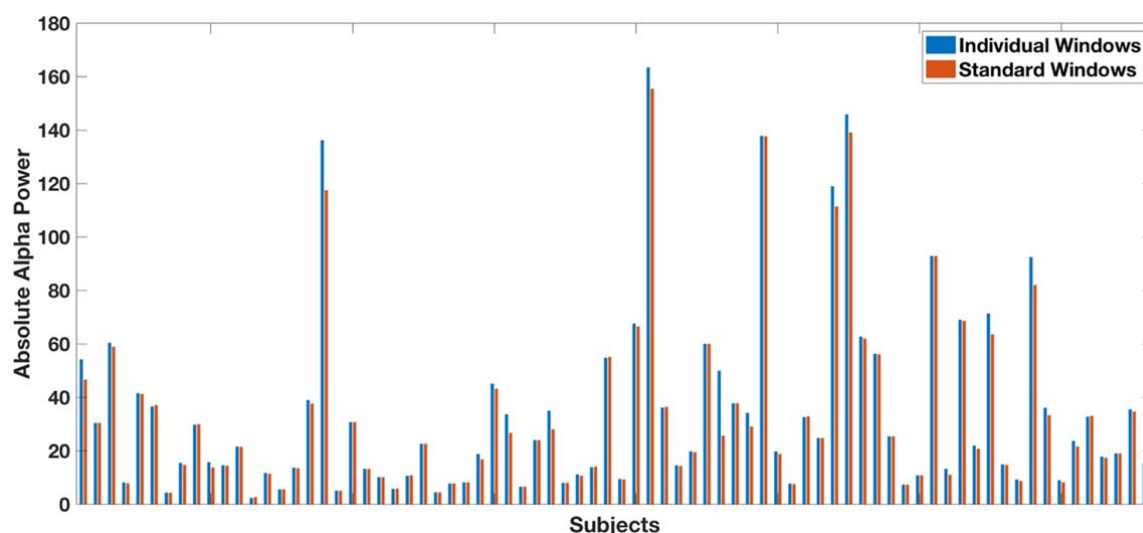
Figure S1. Comparison of Standard Alpha Frequency Windows and Individualized**Windows**

Figure S1. Standard alpha frequency windows of 8-12 Hz were compared with individualized windows, defined as the 4 Hz interval around a midpoint of an individual participant's peak alpha frequency. Absolute parieto-occipital alpha power was almost perfectly correlated across the two methods ($r = .99$, $p < .00001$).

Figure S2. Multilevel Modeling Structure

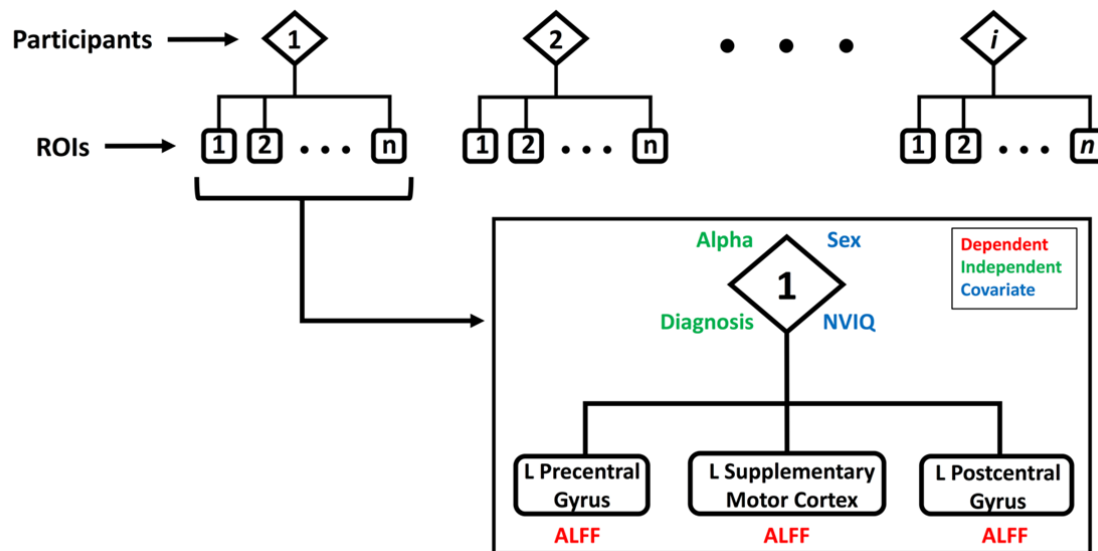


Figure S2. The general hierarchical structure for multilevel models used in this study consists of ROIs nested within subjects. Separate multilevel models were conducted for each functional ROI group, where each of i participants has fMRI data from n ROIs. A multimodal example is provided for a single participant in a model including the left somatomotor ROI group. This participant has three observations of dependent variable ALFF (one per ROI), and one observation of alpha power, diagnosis (independent variables), sex, and NVIQ (covariates).

Figure S3. Alpha Power Group Differences in Unmedicated Subsample

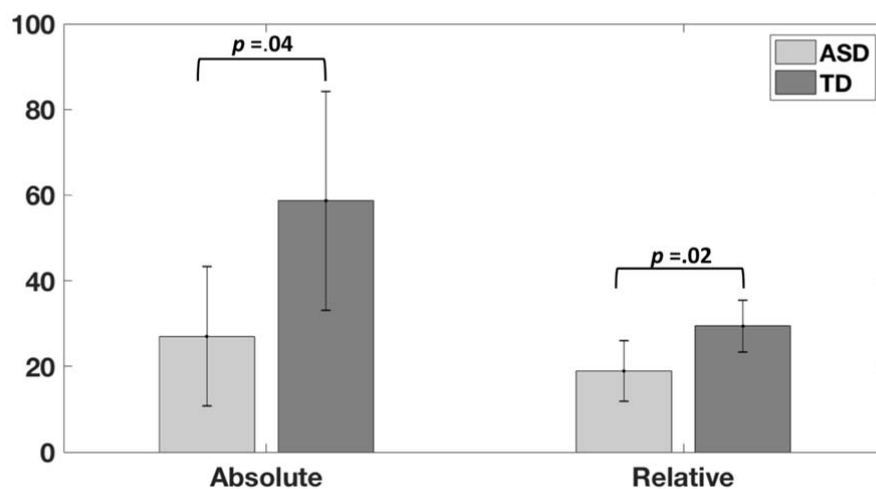


Figure S3. In an unmedicated subsample of ASD participants ($n = 17$) and a matched TD group ($n = 17$), absolute and relative alpha power were smaller in the ASD group than the TD group. These findings corroborate those reported in the main analysis with the full sample of medicated and unmedicated participants.

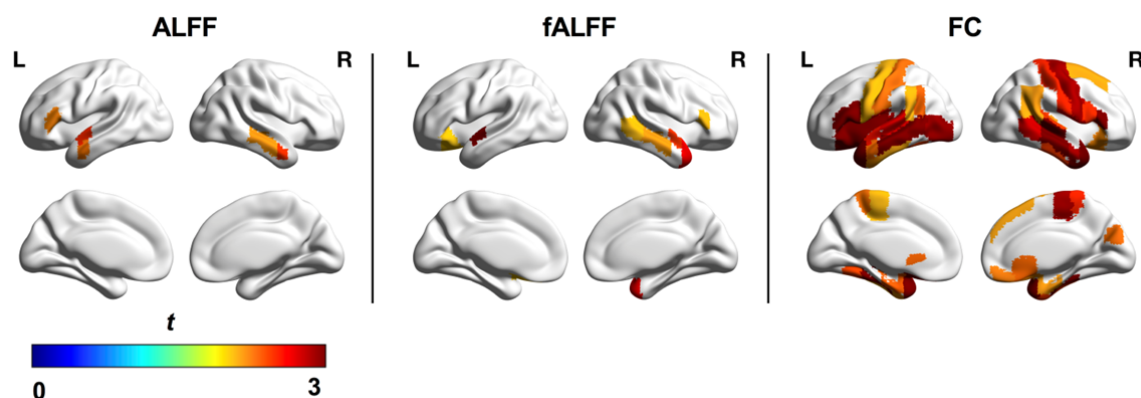


Figure S4. fMRI Group Differences in Unmedicated Subsample

Figure S4. In an unmedicated subsample of ASD participants ($n = 37$) and a matched TD group ($n = 37$), group differences in fMRI measures were similar to those reported in the full sample ($p < .05$, uncorr). Specifically, increased ALFF in right temporal ROIs, increased fALFF in bilateral temporal ROIs, and widespread thalamocortical overconnectivity were found in both the main and supplemental analyses.

Figure S5. Individual ALFF-Alpha Power Relationships by Group

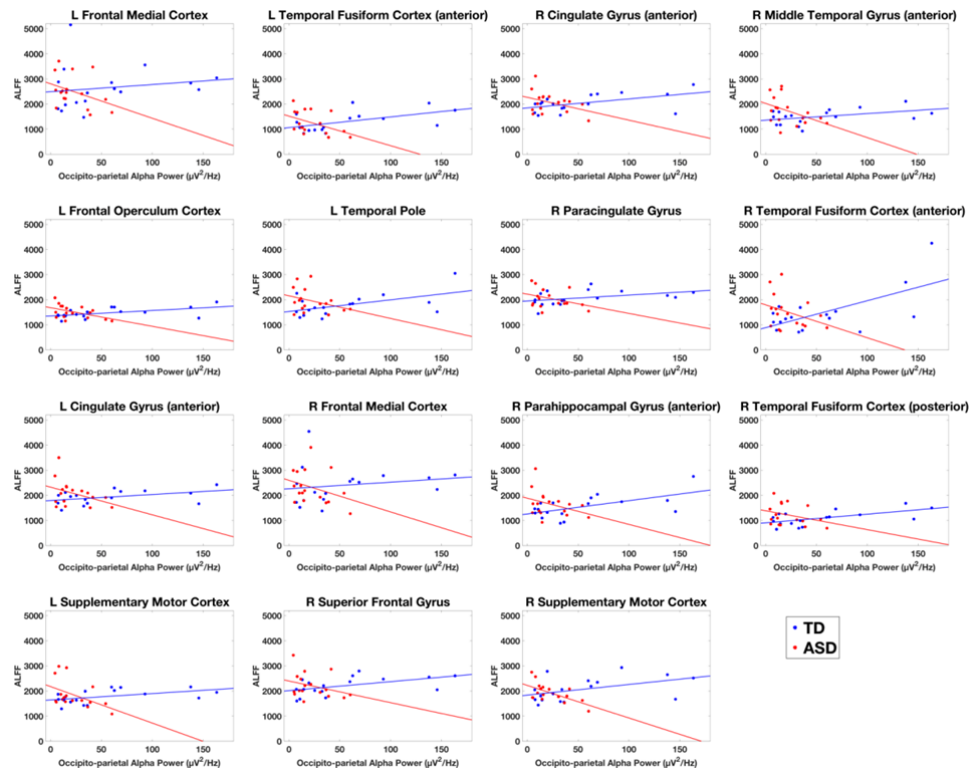


Figure S5. Individual occipito-parietal alpha power is plotted against ALFF and color-coded by group. Scatterplots are only shown for ROIs with significant interactions between diagnosis and alpha power on ALFF in general linear models (i.e., the ALFF-Alpha relationship differs significantly between groups). For these ROIs, the TD group consistently demonstrates a positive relationship between alpha power and ALFF, whereas this association is negative in ASD.